Improved modeling of electrified interfaces using the effective screening medium method

Ikutaro Hamada,[1,*] Osamu Sugino,[2] Nicéphore Bonnet,[2,3] and Minoru Otani[3]

[1]*International Center for Materials Nanoarchitectonics (WPI-MANA), National Institute for Materials Science (NIMS), Tsukuba 305-0044, Japan*

[2]*Institute for Solid State Physics, University of Tokyo, Kashiwa 277-8581, Japan*

[3]*Nanosystem Research Institute, National Institute of Advanced Industrial Science and Technology (AIST), Tsukuba 305-8568, Japan*

(Received 8 June 2013; published 21 October 2013)

An update of the effective screening medium (ESM) method [Otani and Sugino, Phys. Rev. B **73**, 115407 (2006)] is presented, extending the ability to simulate electrified interfaces in an efficient and flexible way. The need for an artificial vacuum buffer between the molecular system and the screening medium is removed by defining a smooth transition of the ESM dielectric permittivity (smooth ESM), precluding numerical instabilities when molecules come in contact with the ESM. Moreover, at short distances, the smooth ESM acts as a repulsive wall, and thus the simulation cell can serve as a natural container for molecules in molecular-dynamics simulations. Consequently, the smooth ESM method is a substantial advancement in modeling solid-liquid interfaces under electric bias.

DOI: 10.1103/PhysRevB.88.155427 PACS number(s): 73.20.−r, 68.08.−p, 31.15.E−

I. INTRODUCTION

There has been a growing interest in simulating electrified interfaces, e.g., the electrochemical double layer, because of their relevance to energy conversion and storage devices, such as fuel cells, solar cells, and batteries. The thickness of the double layer of a water solution is simply estimated to be 1 nm (pH = 1) to 1 μm (pH = 7). This fact hinders first principles treatment of the double layer, and prompts modeling of distant electrolyte ions. In earlier studies, the effect of the electrolyte ions has been incorporated as an external electric field arising from a dipole layer[1] or a charged layer,[2–7] which is located in a vacuum region of electrode/solution/vacuum interface models. Alternatively, an electric field is applied by introducing compensating background charge.[8–10] More recent studies[11–16] have used electrode/solution/continuum interface models, where the continuum is characterized by dielectric constant and/or classical charges. Methods to calculate electrode potential, one of essential quantities in electrochemistry, have also been developed.[10–12,15–19] Among other approaches, the effective screening medium (ESM) method[11] has been developed as a way to simulate electrified interfaces within a first principles framework using periodic boundary conditions (PBC). Given a slab geometry standing for the interface, the ESM method applies a correction that lifts the periodic-boundary condition in the surface normal direction, thereby allowing computation of the electrostatic potential of the isolated slab. Additionally, the method allows filling the region away from the slab with a dielectric screening medium—the ESM *per se*—as a simple way to include electrostatic screening effects of the environment. Because the electrostatic potential is obtained analytically using the Green's function technique, the computational cost is comparable with that of a conventional PBC calculation, opening the way to large-scale molecular-dynamics simulations of electrified interfaces within density functional theory (DFT).[20–25] The method has also been applied successfully to surfaces[26] and molecules[27] isolated in vacuum, in place of the dipole correction.[28,29]

In the original version of the ESM method, the screening medium has a sharp boundary, that is, the relative permittivity changes discontinuously from $\epsilon = 1$ to $\epsilon > 1$ at the boundary located between the vacuum region and the ESM [original ESM, Fig. 1(a)]. The discontinuous change causes numerical instability when the electron density touches the boundary. This is particularly problematic when simulating interfaces between an electrode and a solution, because the molecules of the solution would naturally come in close contact with the ESM. To avoid this problem, a vacuum region has been inserted as a buffer between the molecules and the ESM, and an artificial potential wall has been used to prevent the molecules and electrons from entering the buffer (see, e.g., Refs. 21 and 25). It is important to remove this restriction to better model electrified interfaces.

Here, we improve upon the description of the screening medium by imposing a smooth transition of the dielectric permittivity between the vacuum region and the ESM [smooth ESM, Fig. 1(b)], and thus lift the nonoverlap constraint on the electronic charge density. In line with the approach adopted in the polarizable continuum model of Fattebert and Gygi,[30] the present method models the permittivity by a simple analytical function, varying smoothly from $\epsilon = 1$ to $\epsilon > 1$ at the boundary of the ESM region. The corresponding Green's function, electrostatic potential, and energy are then derived. After implementing this approach into our DFT code and conducting various tests, it turns out that, in case of an overlap with the electronic charge of molecules, the smooth ESM potential is numerically stable and acts naturally as a repulsive wall, thus removing the needs for an artificial vacuum buffer and for an additional potential wall simultaneously.

II. METHOD

In the ESM method, the total energy functional has the following expression,

$$E_{\rm tot}[\rho_{\rm e}] = T_{\rm s}[\rho_{\rm e}] + E_{\rm xc}[\rho_{\rm e}] + \int\int d\boldsymbol{r}d\boldsymbol{r}'\rho_{\rm e}(\boldsymbol{r})G(\boldsymbol{r},\boldsymbol{r}')\rho_{\rm I}(\boldsymbol{r}') + \frac{1}{2}\int\int d\boldsymbol{r}d\boldsymbol{r}'\rho_{\rm e}(\boldsymbol{r})G(\boldsymbol{r},\boldsymbol{r}')\rho_{\rm e}(\boldsymbol{r}') + \frac{1}{2}\int\int d\boldsymbol{r}d\boldsymbol{r}'\rho_{\rm I}(\boldsymbol{r})G(\boldsymbol{r},\boldsymbol{r}')\rho_{\rm I}(\boldsymbol{r}'), \quad (1)$$

 ©2013 American Physical Society

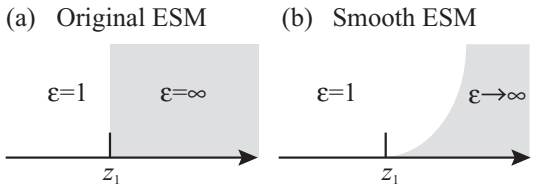

FIG. 1. Schematic views of (a) the original ESM and (b) the smooth ESM. Here, the ESM acts as a metal, hence the infinite permittivity.

where ρ_e and ρ_I are the electronic and ionic charge densities, respectively; T_s is the kinetic energy; E_{xc} is the exchange-correlation energy. The third, fourth, and fifth terms are the electron-ion interaction, Hartree, and ion-ion interaction energies, respectively, and they are expressed in terms of the Green's function $G(\boldsymbol{r},\boldsymbol{r}')$ satisfying Poisson's equation,

$$\nabla \cdot [\epsilon(\boldsymbol{r})\nabla] G(\boldsymbol{r},\boldsymbol{r}') = -4\pi\delta(\boldsymbol{r}-\boldsymbol{r}'). \tag{2}$$

Adopting Laue's representation, the previous equation becomes

$$\{\partial_z[\epsilon(z)\partial_z]\epsilon(z) - g_\parallel^2\} G(\boldsymbol{g}_\parallel,z,z') = -4\pi\delta(z-z'), \tag{3}$$

where $\boldsymbol{g}_\parallel$, with norm $g_\parallel$, is a generic vector of the reciprocal lattice, parallel to the surface, and z is the real-space coordinate in the direction perpendicular to the surface. Moreover, the relative permittivity $\epsilon(z)$ is assumed to be a function of z only.

Considering the case where the screening medium acts as a metal, that is, a medium with an infinite permittivity, we choose the following expression for the permittivity function,

$$\epsilon(z) = \begin{cases} 1 & z < z_1, \\ e^{a(z-z_1)} & z > z_1, \end{cases} \tag{4}$$

where $z = z_1$ is the boundary of the ESM region, and a is a parameter controlling the smoothness of the transition. As required, the permittivity goes to infinity inside the metallic screening region. Alternative functional forms could be introduced for cases where the ESM has a finite permittivity. Substituting the functional form given by Eq. (4) into Eq. (3), and solving for the Green's function, we obtain

$$G(\boldsymbol{g}_\parallel,z,z') = \begin{cases} \frac{2\pi}{g_\parallel} e^{-g_\parallel|z-z'|} - \frac{2\pi\kappa}{a g_\parallel} e^{g_\parallel(z+z'-2z_1)} & (z,z' < z_1) \\ \frac{8\pi}{\alpha} e^{g_\parallel(z-z_1)+\frac{1}{2}\xi(z_1-z')} & (z < z_1 < z') \\ \frac{8\pi}{\alpha} e^{g_\parallel(z'-z_1)+\frac{1}{2}\xi(z_1-z)} & (z' < z_1 < z) \\ -\frac{4\pi\beta}{\alpha\lambda} e^{\frac{1}{2}\xi(2z_1-z-z')} + \frac{4\pi}{\lambda} e^{\frac{1}{2}a(2z_1-z-z')-\frac{1}{2}\lambda|z-z'|} & (z,z' > z_1) \end{cases}$$

where $\alpha = a + 2g_\parallel + \sqrt{a^2+4g_\parallel^2}$; $\beta = a + 2g_\parallel - \sqrt{a^2+4g_\parallel^2}$; $\xi = a + \sqrt{a^2+4g_\parallel^2}$; $\kappa = -2g_\parallel + \sqrt{a^2+4g_\parallel^2}$; $\lambda = \sqrt{a^2+4g_\parallel^2}$. In the limit where $a \to \infty$, it can be shown that the Green's function reduces to

$$G(z,z') = \frac{2\pi}{g_\parallel} e^{-g_\parallel|z-z'|} - \frac{2\pi}{g_\parallel} e^{g_\parallel(z+z'-2z_1)}, \tag{5}$$

which is consistent with the expression obtained for the original ESM scheme, given by Eq. 15 of Ref. 11 for boundary condition (iii) ["vacuum/metal"]. It is moreover apparent, from the obtained Green's function, that the electron-ion and Hartree potentials will be smooth at $z = z_1$.

III. RESULTS AND DISCUSSIONS

The smooth ESM method has been implemented into the STATE[31] code (see Supplemental Material[32] for details), and applied to various test cases reported here. The calculations have been performed with the Perdew-Burke-Ernzerhof functional[33] (PBE) for the electronic exchange-correlation energy, ultrasoft pseudopotentials[34] for the electron-ion interaction, and cutoff energies of 25 and 225 Ry for the plane-wave basis sets of the wave functions and augmentation charge, respectively.

A. CO molecule

In the first set of calculations, a carbon monoxide (CO) molecule is placed in a $0.5 \times 0.5 \times 2.4$ nm^3 unit cell, with its bond in the longitudinal direction (z). The ESM is placed at a distance $z_1 = 1.0$ nm from the center of the unit cell ($z = 0$). The total energy, computed at the Γ point of the Brillouin zone with the CO bond length held fixed, was calculated as a function of the z coordinate of the O atom (z_O). It is plotted in Fig. 2, for different values of the smoothness parameter a, going from 11.34 to 18.90 nm^{-1}. Initially, as the CO molecule approaches the ESM, the total energy decreases owing to the attractive interaction with the image charge induced in the ESM. However, at the point where the tail of the ionic potential starts overlapping with the ESM, the attractive ion-electron interaction gets partially screened and the electronic energy increases, such that the ESM acts as a repulsive wall for the molecule. Moreover, the strength of the repulsion is controlled by the smoothness parameter, that is, the larger the value of a, the stronger the screening of the potential, and thus, the larger the repulsive force. When a is smaller than a certain value, the attractive and repulsive forces balance, and give rise to an energy minimum. Thus, in general, the potential acting on a molecule in the vicinity of the ESM can be tuned by the smoothness parameter a.

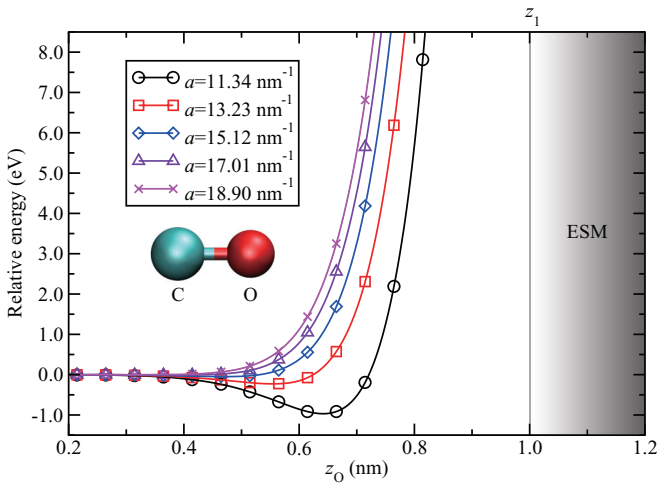

FIG. 2. (Color online) Total energy as a function of the longitudinal position of the CO molecule z_O and for different values of the smoothness parameter a.

B. H_2O molecule

Next, we consider the case of a water molecule in a $1.0 \times 1.0 \times 2.8$ nm^3 unit cell. The position of the ESM is unchanged ($z_1 = 1.0$ nm), and the value of the smoothness parameter is fixed at $a = 5.67$ nm^{-1}. Three configurations of the water molecule are computed: (i) "H-down", in which the H atoms point away from the ESM; (ii) "H-para", in which the molecule lies parallel to the surface; (iii) "H-up", in which the H atoms point toward the ESM. The total energy computed as a function of the longitudinal position of the water molecule (Fig. 3) turns out to be only slightly affected by the specific molecular orientation, and exhibits a minimum around 0.2–0.3 nm, before the onset of the repulsive force.

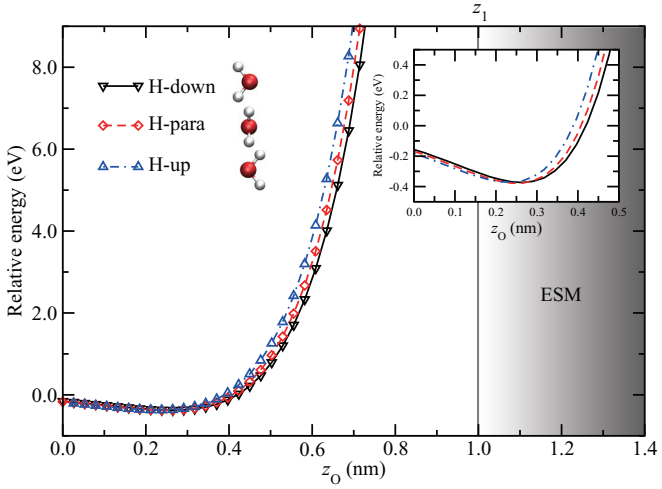

FIG. 3. (Color online) Total energy as a function of the longitudinal position of the water molecule and for different molecular orientations. The inset is an enlargement around the energy minimum. $a = 5.67$ nm^{-1} is used.

C. Metallic slab

Last, the smooth ESM method is used to study the charge and potential of an aluminum electrode under bias. The electrode is modeled by a six-layer Al slab in the (111) direction, with 1×1 unit cell in the xy plane, and a PBE-optimized lattice constant of 0.41 nm. The thickness of the vacuum region around the slab is equivalent to 13 layers (3.27 nm), and the Brillouin zone is sampled using a Γ-centered $8 \times 8 \times 1$ k-point mesh. The ESM is placed at a distance of 0.82 nm from the surface of the slab, and the value of the smoothness parameter is $a = 9.45$ nm^{-1}. The system is put under bias by adding up to ± 0.02 electrons to the slab, and the excess/deficit charge density and potential are plotted (Fig. 4). Owing to the metallic screening, the excess charge density accumulates at the surface of the slab, consistent with the behavior already observed in Ref. 11 using boundary condition (iii) ["vacuum/metal"]. However, a qualitatively different feature appears in the fact that inside the ESM region, the electrostatic potential approaches zero gradually as a result of the smooth permittivity transition, in contrast to the original ESM version, in which the potential is abruptly changed to 0 at $z = z_1$.[11] Moreover, the charge induced in ESM can be calculated as

$$\Delta\rho_{\rm ind}(\boldsymbol{r}) = -\nabla \cdot \boldsymbol{P}(\boldsymbol{r}) = \nabla \cdot \left[\frac{\epsilon(\boldsymbol{r}) - 1}{4\pi} \nabla V(\boldsymbol{r})\right], \quad (6)$$

where $\boldsymbol{P}(\boldsymbol{r})$ and $V(\mathbf{r})$ are polarization and electrostatic potential, respectively. In Fig. 4(d), it can be seen that the image charge is induced in ESM, which screens the electrostatic potential. This demonstrates the role of the smooth ESM.

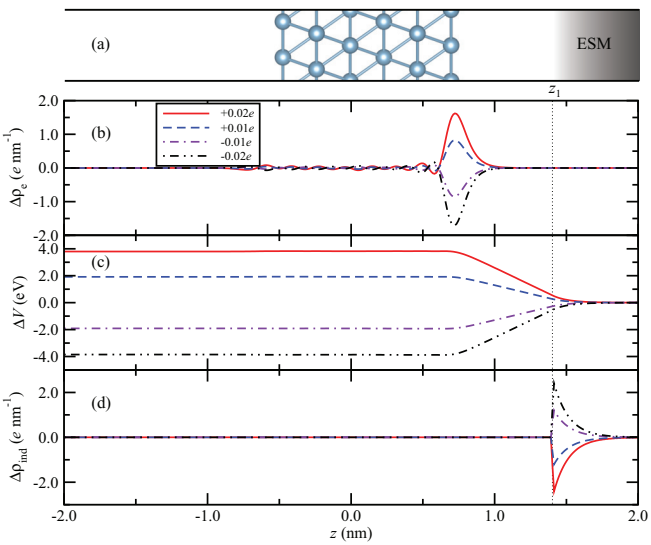

FIG. 4. (Color online) Planar average of electronic charge density difference $\Delta\rho_e$, electrostatic potential difference ΔV, and induced charge in ESM $\Delta\rho_{\rm ind}$, upon charging the slab. (a) Longitudinal view of the setup with the Al(111) slab and the ESM. (b) Electronic charge density difference compared to that of the neutral slab. A positive (negative) sign indicates an excess (deficit) of electrons. (c) Electrostatic potential difference compared to that of the neutral slab. (d) Image charge induced in ESM. The vertical dotted line stands for the surface of the ESM.

IV. SUMMARY

The ESM method has been improved by letting the dielectric permittivity vary smoothly between the vacuum region and the ESM, thereby lifting the need for an artificial vacuum buffer between the molecular system and the ESM. The Green's function has been derived for the new functional form of the permittivity, and implemented into our plane-wave DFT code. Various tests conducted on small molecules have shown that the smooth ESM acts as a repulsive wall at short distances, and that the strength of the repulsion can be tuned by the smoothness parameter of the permittivity. Thus, the smooth ESM is not only a numerically robust screening medium, but it also acts as a natural container wall for molecules in molecular-dynamics simulations, thereby extending the ability to model electrified interfaces in an efficient and flexible manner. By combining the presently upgraded ESM method with a scheme recently developed to perform calculations at a constant electrode potential,[35] we believe that the simulation of solid-liquid interfaces under electric bias can be greatly advanced.

ACKNOWLEDGMENTS

This work was partly supported by a Grant-in-Aid for Scientific Research on Innovative Area "Materials Design through Computics: Complex Correlation and Non-equilibrium Dynamics" from the Ministry of Education, Culture, Sports, Science and Technology (MEXT), Japan (No. 23104501), the Strategic Program for Inovative Research (SPIRE), MEXT, Japan, the Computational Materials Science Initiative (CMSI), Japan, and the World Premier International Research Center Initiative (WPI), MEXT, Japan. Numerical calculations were performed at the Supercomputer Center, Institute for Solid State Physics, University of Tokyo, and at the Information Technology Center, University of Tokyo.

*HAMADA.Ikutaro@nims.go.jp

[1] J. Rossmeisl, J. K. Nørskov, C. D. Taylor, M. J. Janik, and M. Neurock, J. Phys. Chem. B **110**, 21833 (2006).
[2] C. L. Fu and K. M. Ho, Phys. Rev. Lett. **63**, 1617 (1989).
[3] K. P. Bohnen and D. M. Kolb, Surf. Sci. **407**, L629 (1998).
[4] A. Y. Lozovoi and A. Alavi, Phys. Rev. B **68**, 245416 (2003).
[5] J. G. Che and C. T. Chan, Phys. Rev. B **67**, 125411 (2003).
[6] S. Kajita, T. Nakayama, and M. Kawai, J. Phys. Soc. Jpn. **76**, 044701 (2007).
[7] S. Schnur and A. Groß, Catal. Today **165**, 129 (2011).
[8] A. Y. Lozovoi, A. Alavi, J. Kohanoff, and R. M. Lynden-Bell, J. Chem. Phys. **115**, 1661 (2001).
[9] J.-S. Filhol and M. Neurock, Angew. Chem. Int. Ed. **45**, 402 (2006).
[10] C. D. Taylor, S. A. Wasileski, J.-S. Filhol, and M. Neurock, Phys. Rev. B **73**, 165402 (2006).
[11] M. Otani and O. Sugino, Phys. Rev. B **73**, 115407 (2006).
[12] R. Jinnouchi and A. B. Anderson, Phys. Rev. B **77**, 245417 (2008).
[13] I. Dabo, B. Kozinsky, N. E. Singh-Miller, and N. Marzari, Phys. Rev. B **77**, 115139 (2008).
[14] I. Dabo, N. Bonnet, Y. L. Li, and N. Marzari, *Fuel Cell Science: Theory, Fundamentals, and Biocatalysis*, edited by A. Wieckowski, and J. Nørskov (Wiley, New York, 2010), Chap. 13.
[15] K. Letchworth-Weaver and T. A. Arias, Phys. Rev. B **86**, 075140 (2012).
[16] Y. H. Fang, G. F. Wei, and Z. P. Liu, Catal. Today **202**, 98 (2013).
[17] J. Rossmeisl, E. Skúlason, M. E. Björketun, V. Tripkovic, and J. K. Nørskov, Chem. Phys. Lett. **466**, 68 (2008).
[18] V. Tripkovic, M. E. Björketun, E. Skúlason, and J. Rossmeisl, Phys. Rev. B **84**, 115452 (2011).
[19] J. Cheng and M. Sprik, Phys. Chem. Chem. Phys. **14**, 11245 (2012).
[20] O. Sugino, I. Hamada, M. Otani, Y. Okamoto, and T. Ikeshoji, Surf. Sci. **601**, 5237 (2007).
[21] M. Otani, H. Hamada, O. Sugino, Y. Morikawa, Y. Morikawa, Y. Okamoto, and T. Ikeshoji, J. Phys. Soc. Jpn **77**, 024802 (2008).
[22] M. Otani, H. Hamada, O. Sugino, Y. Morikawa, Y. Morikawa, Y. Okamoto, and T. Ikeshoji, Phys. Chem. Chem. Phys. **10**, 3609 (2008).
[23] I. Hamada and Y. Morikawa, J. Phys. Chem. C **112**, 10889 (2008).
[24] T. Ikeshoji, M. Otani, I. Hamada, and Y. Okamoto, Phys. Chem. Chem. Phys. **13**, 20223 (2011).
[25] T. Ohwaki, M. Otani, T. Ikeshoji, and T. Ozaki, J. Chem. Phys. **136**, 134101 (2012).
[26] I. Hamada, M. Otani, O. Sugino, and Y. Morikawa, Phys. Rev. B **80**, 165411 (2009).
[27] Y. Takimoto, M. Otani, and O. Sugino, Phys. Rev B **81**, 153405 (2010).
[28] J. Neugebauer and M. Scheffler, Phys. Rev. B **46**, 16067 (1992).
[29] L. Bengtsson, Phys. Rev. B **59**, 12301 (1999).
[30] J.-L. Fattebert and F. Gygi, J. Comput. Chem. **23**, 662 (2002).
[31] Y. Morikawa, H. Ishii, and K. Seki, Phys. Rev. B **69**, 041403(R) (2004).
[32] See Supplemental Material at http://link.aps.org/supplemental/10.1103/PhysRevB.88.155427 for the implementation of the smooth ESM.
[33] J. P. Perdew, K. Burke, and M. Ernzerhof, Phys. Rev. Lett. **77**, 3865 (1996).
[34] D. Vanderbilt, Phys. Rev. B **41**, 7892 (1990).
[35] N. Bonnet, T. Morishita, O. Sugino, and M. Otani, Phys. Rev. Lett. **109**, 266101 (2012).